frontiers | Frontiers in Environmental Science

TYPE Original Research
PUBLISHED 31 January 2025
DOI 10.3389/fenvs.2025.1522700

Amorphous silica reduces N_2O emissions from arable land at the field plot scale

Mathias Hoffmann[1], Oscar Rodrigo Monzon Diaz[1], Isabel Zentgraf[2], Wael Al-Hamwi[1], Maren Dubbert[1], Mathias Stein[3], Maire Holz[2†] and Jörg Schaller[3,4*†]

[1]Leibniz Center for Agricultural Landscape Research (ZALF), Working Group for Isotope Biogeochemistry and Gas Fluxes, Müncheberg, Germany, [2]Leibniz Center for Agricultural Landscape Research (ZALF), Working Group for Root Soil Interaction, Müncheberg, Germany, [3]Leibniz Center for Agricultural Landscape Research (ZALF), Working Group for Silicon Biogeochemistry, Müncheberg, Germany, [4]FB 09 Agrarwissenschaften, Ökotrophologie und Umweltmanagement, University of Gießen, Gießen, Germany

Check for updates

OPEN ACCESS

EDITED BY
Wei Lin,
Chinese Academy of Agricultural Sciences (CAAS), China

REVIEWED BY
Rui Yang,
Chinese Academy of Agricultural Sciences, China
Hong Wang,
Chinese Academy of Agricultural Sciences, China

*CORRESPONDENCE
Jörg Schaller,
Joerg.Schaller@zalf.de

†These authors have contributed equally to this work and share senior authorship

RECEIVED 04 November 2024
ACCEPTED 10 January 2025
PUBLISHED 31 January 2025

CITATION
Hoffmann M, Diaz ORM, Zentgraf I, Al-Hamwi W, Dubbert M, Stein M, Holz M and Schaller J (2025) Amorphous silica reduces N_2O emissions from arable land at the field plot scale.
Front. Environ. Sci. 13:1522700.
doi: 10.3389/fenvs.2025.1522700

Introduction: Increasing greenhouse gas emissions pose a strong threat due to accelerating global warming. N_2O emissions are highly important in this regard as N_2O is a very powerful greenhouse gas. Agriculture is the main human-induced source for N_2O emissions, contributing roughly 60% to total N_2O emissions. Soil amorphous silica (ASi) contents are reduced in arable soils due to yearly exports by crop harvest as most crops are silicon accumulator plants. Most recently it has been shown that ASi is increasing water and nutrient availability in soils. Both factors are known to directly and indirectly affect N_2O emissions from agroecosystems.

Methods: In this study we conducted a field plot trial on arable soil depleted in ASi and fertilized this soil to its pre-agricultural ASi level.

Results: Our data clearly shows that increasing soil ASi to a pre-agricultural level decreased seasonal N_2O emissions by ~30%.

Discussion: This reduction of N_2O emissions due to ASi might be of global relevance as agricultural practice has reduced the ASi content in agricultural soils. If future studies confirm the effect of ASi on N_2O emissions, the soil ASi depletion by agricultural practice in the last decades may have led to a substantial increase of N_2O emissions.

KEYWORDS

agriculture, crop production, greenhouse gas, nitrogen cycle, silicon

1 Introduction

Nitrogen (N) is the nutrient that most often limits productivity of terrestrial ecosystems (Vitousek and Howarth, 1991; LeBauer and Treseder, 2008) though excess N has various negative consequences for the environment (Sutton et al., 2011) such as production of greenhouse gases and leaching of nitrate (NO_3^-) into groundwater (Galloway et al., 2013; Van Groenigen et al., 2015). Soil N transformations and losses are controlled by several, microbial mediated and simultaneously occurring processes (Myrold and Tiedje, 1986; Hart et al., 1994). The amount of N that is available for plant uptake is determined by the balance between microbial transformation of soil organic N (SON) to soil mineral N and the microbial immobilization of soil mineral N (Hart et al., 1994; Liu et al., 2019). In agricultural systems, mineralized ammonium (NH_4^+) is rapidly transformed into nitrate (NO_3^-) during nitrification, a process during which nitrous oxid (N_2O) is produced as a side product. Additionally, N_2O production occurs when nitrate undergoes denitrification (Norton and Schimel, 2011). N_2O production is a major concern within the N cycle because N_2O is both a powerful greenhouse gas (Badr and Probert, 1993) as well as the main contributor to destruction of stratospheric ozone (Ravishankara et al., 2009).

Agriculture stands out as the primary human-induced source contributing to the escalating concentration of atmospheric N_2O, accounting for roughly 60% of the total N_2O emissions (IPCC, 2013; Mbow et al., 2019). The increasing global demand for food, fodder, and fuel is driving higher N_2O emissions through intensified agricultural practices that involve a growing reliance on both mineral and organic N fertilizers (Reay et al., 2012; Pradhan et al., 2015; Lassaletta et al., 2016). The rate of N_2O emission is closely tied to the quantity of N fertilization. As N fertilization rises, so does the concentration of ammonium (NH_4^+) and nitrate (NO_3^-) in the soil. Those substrates are crucial for microbial processes like nitrification and denitrification, which play a pivotal role in N_2O formation (Bouwman et al., 2002; Shcherbak et al., 2014; Pareja-Sánchez et al., 2020). Additionally, high N_2O emissions are favored in low pH, high C availability, high temperatures and high moisture levels (60%–70% WFPS) (Butterbach-Bahl et al., 2013).

It has recently been shown that amorphous silica (ASi) can significantly reduce water stress under drought conditions, increasing soil moisture. Particularly, Schaller et al., 2020a; Schaller et al., 2020b) showed that ASi significantly enhances soil water holding capacity and water availability, both enabling better plant performance (Schaller et al., 2021b). Soils used for agriculture are depleted in ASi, with natural soils exhibiting an ASi content between 1% and 6% (dry weight) whereas agricultural soils exhibiting an ASi content always below 1% and in most cases zero (Schaller et al., 2021a). This depletion occurs because most crops are Si-accumulators (uptake of monosilicic acid and accumulation of ASi >1% in biomass) (Ma and Takahashi, 2002; Katz et al., 2021) and large amounts of ASi are removed from the fields during harvest (Puppe et al., 2021). A difference in ASi content of just 1% is responsible for a change in the amount of water available to plants by up to 40% as higher ASi contents will lead to higher water holding capacities and therefore more plant available water (Schaller et al., 2020a). The increase in soil water availability by ASi can be explained by a very high water holding capacity of ASi forming silica gels (Schaller et al., 2020a). Additionally, ASi was shown to enhance mobility of soil C and N, as silicic acid competes with C and N for binding at the surface of soil particles (Reithmaier et al., 2017). Both, the increase in water availability but also the increase in soil C and N availability caused by ASi fertilization is likely to affect the release of N_2O from soil. This impact is anticipated to be more noticeable, especially in sandy soils characterized by low water holding capacities, prevalent in the northeast region of Germany. If ASi fertilization results in substantial increases in soil water content, reaching levels conducive to N_2O emissions, it is reasonable to anticipate that ASi fertilization promotes N_2O emissions. Furthermore, the augmented availability of C and N resulting from ASi fertilization may contribute to an increase in N_2O emissions. Conversely, ASi fertilization can improve plant growth by optimizing water conditions. This enhanced growth increases N uptake, which reduces available N and, consequently, N_2O emissions.

Up to date, it has not been investigated to which extent ASi addition to the soil affects soil N cycling and N_2O emissions. We therefore conducted a field trial during 2023/2024 to assess N_2O emissions in barley following fertilization (covering a growing and non-growing season period), comparing plots with and without the addition of ASi. We hypothesized that i) ASi fertilization supports favorable microclimatic conditions through increasing soil moisture, ii) ASi fertilization reduces the available N, and consequently N_2O emission, by increasing crop N uptake during the crop growth period; iii) Depending on which effect dominates, N_2O emissions are increased or decreased under ASi fertilization.

2 Materials and methods

2.1 Study site and experimental design

The study site is located near the city of Müncheberg in NE Germany (52.5176° N, 14.1300° E), at the experimental fields of the Leibniz-Centre for Agricultural Landscape Research (ZALF). The climate is characterized as temperate, with a mean annual air temperature and precipitation of 9.9°C and 509 mm, respectively (ZALF weather station, 2010–2024). The highly heterogeneous soil pattern in this area has been developed from aeolian and glaciofluvial sands overlying a thin layer of glacial till. Due to the strongly variable, upper boundary of the clay-enriched Bt horizon (80–120 cm), soils classified either as Albic Luvisol (Arenic, Aric, Neocambic) or as Albic, Lamellic Arenosol (Aric). The soil texture of the at least upper 80 cm is dominated by medium and fine sand with intercalated clay lamellae of 2–4 cm thickness (Schaller et al., 2021b). In 2020, in total six plots (3 × 4 m^2 100) have been established in a strip design on one of the experimental fields, representing a onetime ASi incorporation treatment to refill the depleted soil silica content (1%ASi (Aerosil 300, Evonik Industries, Germany) incorporated into the plough horizon (30 cm depth) by cultivating (see Schaller et al. (2021b) for details); each (n = 3) and a control (n = 3). Soil characterization of the experimental field (18 × 6 m^2) is given in Table 1. To investigate the effect of ASi fertilization on N_2O emissions during both the growing and non-growing period, weekly N_2O emission measurements were performed for the control and 1% ASi treatment for rainfed spring barley (*Hordeum vulgare* L.; variety: Planet) during the 2023 crop growth period and the subsequent fallow period of 2023/2024. Since ASi incorporation in 2020, spring wheat (2x) and potatoes have been cultivated on the same plots. After seed bed preparation on 21.03.2023 using a full turn plow (plowing depth: 23 cm), spring barley was sown (361 grains per m^2; row distance: 12.5 cm) in all plots on 30.03.2023 using a top-mounted seed drill with rotary harrow. Fertilization with N and sulfur was done at tillering (85 kg ha^{-1} for N and 20 kg ha^{-1} a^{-1} for sulfur) and at heading stage (40 kg ha^{-1} and 10 kg ha^{-1} a^{-1} for sulfur) each PIASAN-S 25/6 (SKW Piesteritz, Germany). Fertilizer application was done using a trailed sprayer with a five-nozzle system (HARDI Ranger Pro VHP, HARDI, Denmark). To protect the plants against herbivory all plots were covered with a fleece until crop emergence (12/04/2023) and treated against weeds with Ariane ™ C (1.5 L ha^{-1}) at stem extension stage.

TABLE 1 Cumulative soil N_2O and CO_2 emissions, total crop biomass and grain yield, crop N, P and Si uptake (summer 2023) as well as soil mineral N, available P, total carbon (C_t), total nitrogen (N_t), and pH (summer 2023 and winter 2023/2024). Given uncertainty represents calculated uncertainty estimates (N_2O and CO_2) as well as ±SE.

Period	Treatment	Soil GHG efflux		N2O intensity	Agronomic WUE	Biomass					Soil							
		g N_2O-N ha^{-1}	t CO_2-C ha^{-1}	mg N_2O g^{-1} grain yield	g grain yield m^{-2} mm^{-1}	DM g m^{-2}	Yield g m^{-2}	N uptake g m^{-2}	P uptake g m^{-2}	Si uptake mg m^{-2}	Bulk density g cm^{-3}	GWC %	Ct %	Nt %	Pcal mg kg^{-1}	pH	NH_4-N_{CaCl2} mg/100 g	NO_3-N_{CaCl2} mg/100 g
Summer	Control	266.6 ± 41.6	1.4 ± 0.3	5.6	1.2	427.5.2 ± 152.4	208.8 ± 76.2	6.7 ± 2.4	1.0 ± 0.3	0.5 ± 0.2	1.5 ± 0.08	5.2 ± 0.09	5.6 ± 0.14	0.6 ± 0.01	45.4 ± 0.7	5.7 ± 0.03	5.8 ± 0.73	8.31 ± 0.76
	ASi	181.9 ± 28.9	2.0 ± 0.3	1.2	2.9	1,069.5 ± 300.0	527.2 ± 161.3	15.0 ± 4.9	2.5 ± 0.7	4.4 ± 1.9	1.6 ± 0.06	4.7 ± 0.31	4.3 ± 0.04	0.5 ± 0.01	55.6 ± 0.8	5.3 ± 0.06	13.53 ± 0.57	11.43 ± 0.06
	Effect size (d)	−2.36	2.00	—	—	2.70	2.52	2.15	2.79	2.89	−0.7	−2.06	−12.36	−10.00	13.57	−8.43	11.8	5.79
	p-value	>0.1	>0.1	—	—	≤0.1	≤0.1	≤0.1	≤0.1	≤0.1	>0.1	>0.1	>0.1	>0.1	>0.1	>0.1	>0.1	>0.1
Winter	Control	25.6 ± 7.5	0.3 ± 0.1	—	—	—	—	—	—	—	—	9.2 ± 0.24	5.15 ± 0.18	0.5 ± 0.04	43.8 ± 0.6	5.1 ± 0.08	0.11 ± 0.04	0.04 ± 0.01
	ASi	25.8 ± 6.3	0.2 ± 0.0	—	—	—	—	—	—	—	—	9.5 ± 0.47	4.2 ± 0.39	0.4 ± 0.04	51.4 ± 1.5	4.6 ± 0.1	0.08 ± 0.01	0.03 ± 0.01
	Effect size (d)	0.03	−0.94	—	—	—	—	—	—	—	—	0.72	−2.77	−2.50	5.81	−5.28	−1.30	−1
	p-value	>0.1	>0.1	—	—	—	—	—	—	—	—	>0.1	≤0.05	≤0.05	≤0.05	≤0.05	>0.1	>0.1

10.3389/fenvs.2025.1522700

2.2 Soil and plant and analyses

Soil samples were collected at ASi fertilization (18/03/2020), at 20/06/2023 and at 29/01/2024 (depth 0–15 cm). Soil samples were taken randomly at five locations within each plot using an auger (diameter 5 cm), avoiding field and treatment borders. Soil samples were subsequently analyzed for mineral N (NH_4^+ + NO_3^-) (VDLUFA MB Bd. 1 Kap. 6.1.4.1, CFA-SAN, Skalar GmbH, Germany) at the central laboratory of ZALF. To determine aboveground biomass and grain yield, three biomass samples from an area of 0.4 m × 0.4 m (0.16 m^2) were collected for each treatment at the end of the crop growth period. Each sample was separated for straw and grain, weighed to obtain fresh weight, and oven dried at 50°C for 48 h to determine dry weight. Dried biomass samples were subsequently analyzed for N_t DIN-ISO-10694 (1995), CNS928-MLC, Leco Instruments GmbH, Germany) at the central lab of ZALF. Initial soil ASi content was analysed using 0.1 M Tiron (4,5-dihydroxy-1,3-benzenedisulfonic acid (disodium salt), $C_6H_4Na_2O_8S_2$; Roth, Karlsruhe, Germany) as extractant (Kendrick and Graham, 2004). Plant Si was extracted from 0.03 g biomass samples using 30 mL Na_2CO_3 at 85°C for 5 hours and filtrated at pore-size of 0.2 mm (Puppe et al., 2023). For P analysis, 0.1–0.2 g biomass samples was digested in a closed vessel microwave digestion system (CEM-Mars5, CEM Corporation, Matthews, NC, United States) at 180°C with 3 mL HNO_3 and 2 mL H_2O_2. Si and P concentrations in the extracts were measured at an ICP-OES (Varian, Vista-Pro radial, Palo Alto, California, United States).

2.3 N_2O and CO_2 flux measurements and flux calculation

N_2O and CO_2 fluxes were measured using a non-flow-through non-steady-state (NFT-NSS) manual closed chamber system (Livingston and Hutchinson, 1995). The round (Ø: 16 cm) opaque PVC chambers had a volume of 0.005 m^3 and covered a basal area of 0.02 m^2. To assure airtight closure and prevent leakage, chambers were sealed at the bottom using rubber gaskets. A pressure vent was installed on top of each chamber. Due to the rather small volume and height, chambers were not ventilated, assuming a sufficient headspace homogenization during chamber closure (Hoffmann et al., 2018). A closable valve at the top of the chamber allowed the mounting of pre-evacuated glass bottles (volume: 60 mL) for air sampling. We performed N_2O and CO_2 flux measurements in parallel for all six plots (three per treatment) by deploying the chambers on a PVC frame inserted 5 cm deep into the soil. Chambers were opaque and no plants were present in the small area covered with the frames for N_2O flux measurements. For both measurement periods, frames were installed at least 3 days prior to the first measurement, to ensure a sufficient connection between the frame and the surrounding soil (Charteris et al., 2020). Chamber deployment time was 45 min (Chadwick et al., 2014), with gas samples taken twice per chamber measurement, once at the beginning and once at the end of each measurement. Hence, 6 gas samples were taken per treatment (12 in total) during one measurement campaign. Measurement campaigns were carried out once to twice a week throughout both the crop growing as well as non-growing period. Additional measurement campaigns were conducted to more accurately cover events with expected peaks in N_2O fluxes [50], including multiple N_2O and CO_2 flux measurements per week following mineral N fertilization, as well as after heavy rain and frost-thaw events. Collected gas samples were analyzed for N_2O and CO_2 concentrations using a gas chromatograph (GC-14A and GC-14B, Shimadzu Scientific Instruments, Japan), coupled with an electron capture detector (Loftfield et al., 1997). Resulting N_2O concentrations were subsequently checked for reliability using an expected CO_2 concentration increase (opaque chamber; ecosystem respiration) during chamber closure as a quality criterion. In the case of a non-positive (<0 ppm) CO_2 concentration increase during chamber closure, measurements were considered biased and excluded from further analysis. Finally, N_2O and CO_2 fluxes (F; μmol m^{-2} s^{-1}) were calculated according to the ideal gas law (Equation 1) and based on the often-used assumption of a linear concentration increase during chamber closure [50,52,53].

$$F = pV/RTA \times \Delta c/\Delta t \quad (1)$$

where p represents ambient air pressure (Pa), V denotes chamber volume (m^3), R is the gas constant (8.314 m^3 Pa/K mol^{-1}), T denotes air temperature (K), A represents chamber basal area and dc/dt denotes the N_2O or CO_2 concentration change in chamber headspace over measurement time. N_2O and CO_2 emission estimates were derived through simple linear interpolation of measured N_2O and CO_2 fluxes, thus assuming a linear change between fluxes of two consecutive measurement campaigns. Emission estimates were derived through unit conversion of measured N_2O and CO_2 fluxes (μmol m^{-2} s^{-1}) to g ha^{-1} d^{-1}. Subsequently, daily emissions were linear interpolated, assuming a linear change between fluxes of two consecutive measurement campaigns.

Agronomic water use efficiency (AWUE) was calculated as the ratio of yield (g m^{-2}) to total precipitation (mm) during the growing season Tallec et al. (2013). N_2O intensity was determined following Mosier et al. (2006) through dividing the cumulative N_2O emission (mg m^{-2}) by yield (g m^{-2}).

2.4 Auxiliary measurements

Nearby the experimental field, a weather station measured air temperature in 2 m height, wind speed and direction, relative humidity, air pressure, global radiation, and precipitation in an hourly interval. Additionally, microclimate loggers (TMS-4, TOMST, Czech Republic) were placed next to each frame for soil humidity and temperature, as well as air temperature measurements in a 15 min frequency throughout both measurement periods with measurement depth of 0–8 cm. Plant development stages were visually determined during crop management measures.

2.5 Statistical analysis

After testing for normal distribution using the Kolmogorov-Smirnov test ($p < 0.05$), significant differences in campaign-wise averaged N_2O and CO_2 fluxes between control and ASi plots were determined through performing paired two sample Wilcoxon-tests.

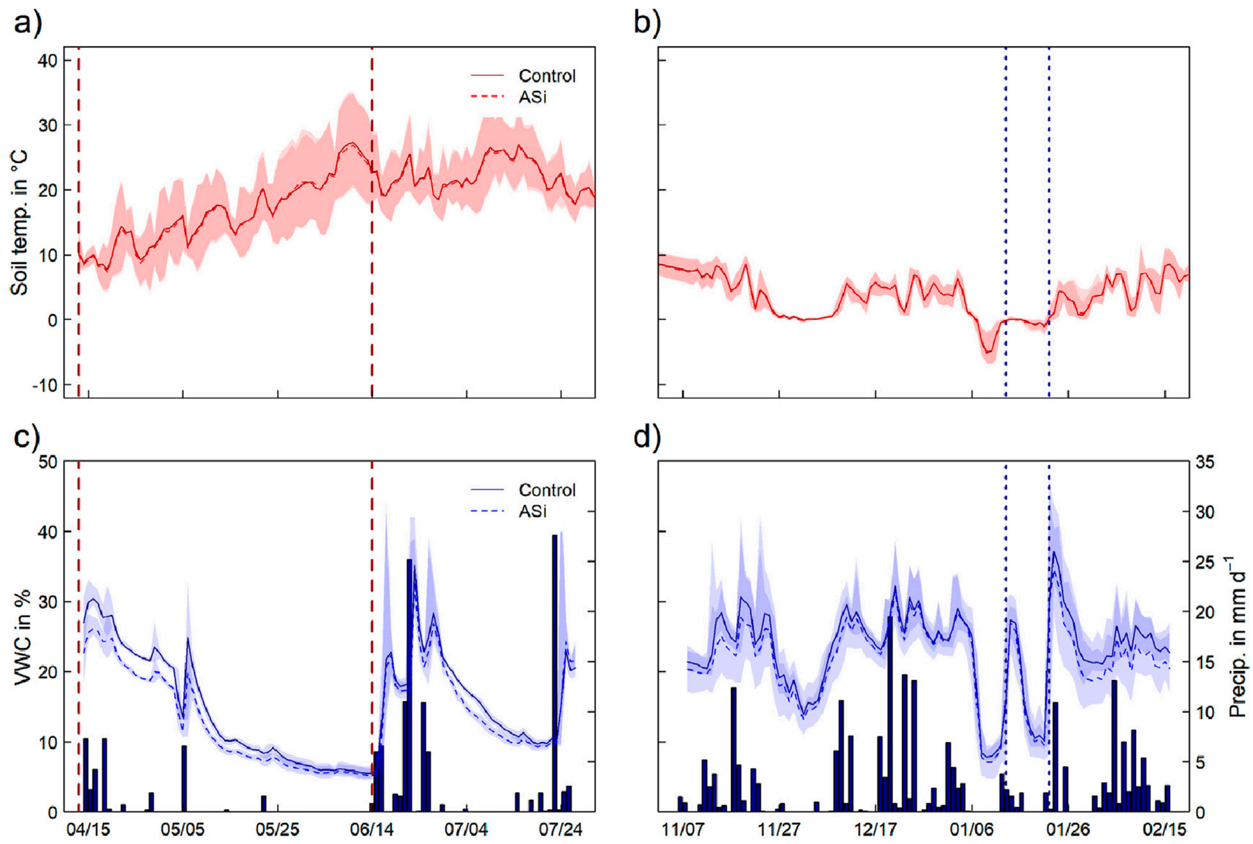

FIGURE 1
Course of soil temperature (°C; solid red line for C and dashed red line for Si) at 6 cm soil depth **(A,B)**, soil moisture (volumetric water content (VWC) in %; solid blue line for C and dashed blue line for Si) and precipitation (mm d^{-1}) **(C,D)** for the crop growth and following fallow period in 2023 **(A,C)** and 2023/2024 **(B,D)** at the study site in Müncheberg. Dashed red vertical lines indicate the two fertilization events. Dotted blue lines represent soil thawing. Shaded areas represent the daily magnitude of measured soil temperature and soil moisture.

The same tests were performed to test for significant differences between obtained biomass and soil parameters. In addition, effect sizes for the comparisons between ASi and Control were calculated using Cohen´s d, where values >0.2, >0.5 and >0.8 indicate a small, medium and strong effect, respectively. We estimated the uncertainty of the measured N_2O and CO_2 emissions by using the error prediction algorithm described in detail by Huth et al. (2018). All statistical analyses were performed using R 4.2.2.

3 Results

3.1 Environmental conditions

Environmental conditions at the study side during the crop growth period in 2023 and following fallow period 2023/2024 are shown in Figure 1. Both periods were characterized by an in average warmer air temperature (>2°C), when compared to the long term average of 15°C for the crop growth period and 2.1°C for the fallow period. During the crop growth period air and soil temperature followed a clear seasonal trend with increasing temperature from April till June and July. During the fallow period, air and soil temperature remained relatively stable with two distinct frost-thaw events occurring consecutively between the 6th and 26th of January 2023. With a precipitation totaling 198.0 mm and 249.2 mm during the crop growth and fallow period respectively, it is notable that only the fallow period experienced significantly higher rainfall compared to the long term average (2000-2020, ZALF), with in average 210.3 mm and 143.9 mm for the respective periods. While precipitation during the winter period was relatively evenly distributed, the crop growth period was primarily characterized by distinct heavy precipitation events (>30 mm per day). These heavy precipitation events coincided with times of fertilization in mid-April and June 2023 and were followed by periods of drying. This erratic pattern is particularly evident in the course of soil moisture development (Figure 1C). Compared to that, the development of soil moisture during the fallow period was relatively stable. However, strong changes in soil moisture was observed during frost, likely attributed to a decrease in soil moisture as water in not available in frozen under these conditions (Figure 1D). During both periods, measurements with the microclimate loggers (Figure 1C) next to each frame revealed that ASi was significantly warmer (<0.25°C; paired *t*-test: p-value <0.01) and less wet (VWC; <2%; paired *t*-test: p-value <0.01) than Control. The initial soil ASi content (control treatment) was 0.2%.

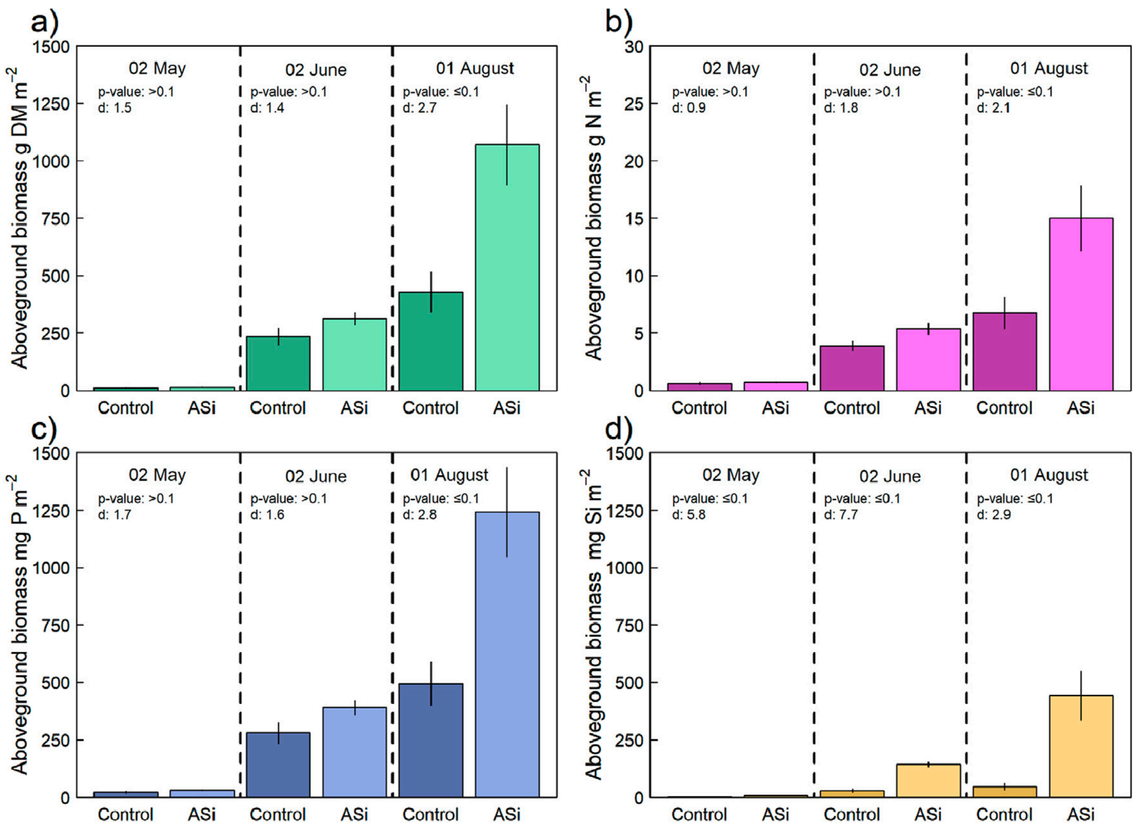

FIGURE 2
Results of the three biomass sampling campaigns (02/05/2024, 02/06/2024 and 01/08/2024) during the crop growth period 2023 with **(A)** barley biomass yield [g dry mass (DM) m^{-2}] and nutrient uptake for **(B)** N (g N m^{-2}), **(C)** P (mg P m^{-2}) and **(D)** silica (Si; mg Si m^{-2}). Error bars indicate ±SE.

3.2 Crop yield, nutrient uptake and soil properties

Total crop biomass and grain yield were substantially higher for ASi fertilized plots (1070.0 ± 173.2 g DM m^{-2} and 527.5 ± 93.1 g DM m^{-2}) than control plots (427.5 ± 88.0 g DM m^{-2} and 210.0 ± 44.0 g DM m^{-2}) (Table 1). Similar differences between ASi and control were observed in the total crop N and P uptake due to only a slightly higher N and identical P concentration in biomass sampled for the control (Nt: 1.6%; P: 0.23%) compared to ASi (Nt: 1.4%; P: 0.23%). In case of Si content in straw, substantial differences were found between both treatments, with the control evidencing a Si content of near zero and ASi showing an Si content of 8.36 mg Si g^{-1} (Table 1). A near zero Si content was found in either of both grain biomass samples.

Figure 2 shows the results of the three biomass sampling campaigns for total crop biomass, as well as crop N, P and Si uptake. No difference in total crop biomass and nutrient uptake was found during the beginning of the crop growth period on 02.05.2024. However, during the following biomass sampling campaigns on 02.06.2024 and 01.08.2024 increasing differences in total crop biomass and nutrient uptake were observed between the control and ASi.

No differences were found in the case of soil mineral N (NH_4-N and NO_3-N), sampled during February 2024 at the end of the fallow period (Table 1).

3.3 Soil N_2O and CO_2 emissions

Temporal dynamics of N_2O (n = 198) and CO_2 emissions (n = 198) during the crop growth and following fallow period measured for the ASi and control treatment, respectively, are shown in Figures 3, 4. During the crop growth period, two distinct N_2O emission peaks were observed, following the first and second N fertilization event in the beginning of April and mid of June 2023 (Figure 3A). During the fallow period, relatively stable N_2O emissions were observed for ASi, while a slight increase in N_2O emissions was observed for C following the first and second frost-thaw events in January 2024 (Figure 3B). While cumulative N_2O emissions for the ASi treatment were more than 30% lower than for the control treatment during the plant growth period, significant differences between observed N_2O fluxes of both treatments were not obtained for the entire measurement duration but only during certain periods. In detail, N_2O emissions measured for both treatments only periodically differed significantly during both the crop growth and fallow period. Thus, N_2O emissions in the ASi-treatment were lower than in the control treatment approx. 3–4 weeks after fertilization and generally slightly higher compared to the control treatment during the fallow period before the first frost-thaw event (Figures 3C, D).

During the crop growth period, CO_2 emissions exhibited a distinct seasonal trend, with substantially higher emissions as compared to the following fallow period (Figures 4A, B). Similar

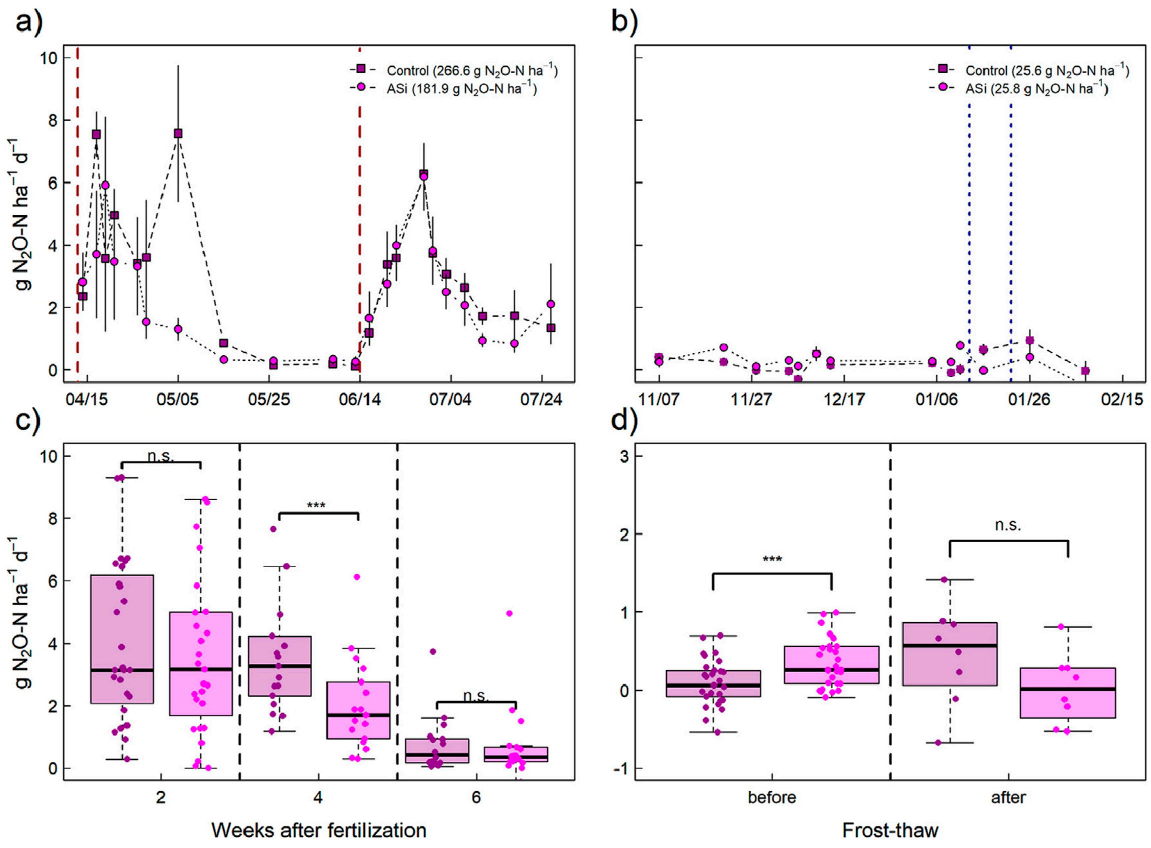

FIGURE 3
Results of periodically measured N_2O emissions (g N_2O-N ha^{-1} d^{-1}) for C (light violet dots) and Si (dark violet dots) during the **(A)** crop growth and **(B)** following fallow period in 2023 and 2023/2024, respectively. Error bars indicate ±SE. **(C, D)** shows boxplots of N_2O emissions grouped by period after fertilization (summer period) and before vs. after frost-thaw (winter period). Significant differences (Wilcoxon-test) between the Treatments within each group are indicated by asterisks (p-value: *** <0.01, ** <0.05, * <0.1, n. s. > 0.1).

to observed N_2O emissions, CO_2 emissions were in general not significantly different between the ASi fertilized and control plots throughout the entire duration of the experiment. Hence, persistently higher, and significantly different CO_2 emission for ASi compared to the control were only found 3–4 months after planting of barley in early April 2023 (Figure 4C). Unlike for N_2O, no significant differences were observed for CO_2 emissions measured before the first and second frost-thaw event for control and ASi during the fallow period. After the frost-thaw events, however, slightly higher CO_2 emissions were obtained in case of ASi during January and February 2024 (Figure 4D).

4 Discussion

We found a reduction of more than 30% cumulative N_2O emissions for the ASi treatment compared to the control treatment at the field plot scale during the plant growth period, accompanied by increased crop N-uptake following ASi fertilization (Figures 2, 3). This confirms our hypothesis that ASi fertilization reduces N_2O emission during the crop growth period, due to an increased crop N uptake, which likely reduced the available N in the soil. Such reduction of N_2O emissions due to ASi addition are of global relevance as agricultural practice has reduced the ASi content in agricultural soils by this 1% (Saccone et al., 2007; Clymans et al., 2011; Schaller et al., 2021a). Hence, the ASi treatment represents soil ASi contents of natural soils not been used for agriculture. If future studies confirm this ASi effect on N_2O emissions, the soil ASi depletion by agricultural practice may have led to substantial increases of N_2O emissions.

ASi fertilization likely reduces N_2O emissions through a combination of mechanisms, including improved plant nutrient and water uptake due to its modification of soil properties. Firstly, it is known that ASi addition enhances plant-available water content in soil (Schaller et al., 2020a). The soil water content in turn plays a critical role in plant nutrient accessibility as nutrient transport within the soil and towards plant roots occurs through mass flow and diffusion (Marschner, 2003), both being demonstrably influenced by soil water content (Seiffert et al., 1995; Zarebanadkouki et al., 2019). Therefore, ASi fertilization, can be expected to accelerate nutrient transport via these mechanisms and to promote nutrient availability for plant uptake. This would be the case in principle for all soil nutrients and has been shown in this study for N and P whose uptake rates were higher under ASi fertilization compared to the control. Secondly, it has to be considered that N mineralization, the process controlling soil N availability, is microbial driven (Hart et al., 1994; Zhang et al., 2018) and as such, it strongly depend on the soil water status. Water stress

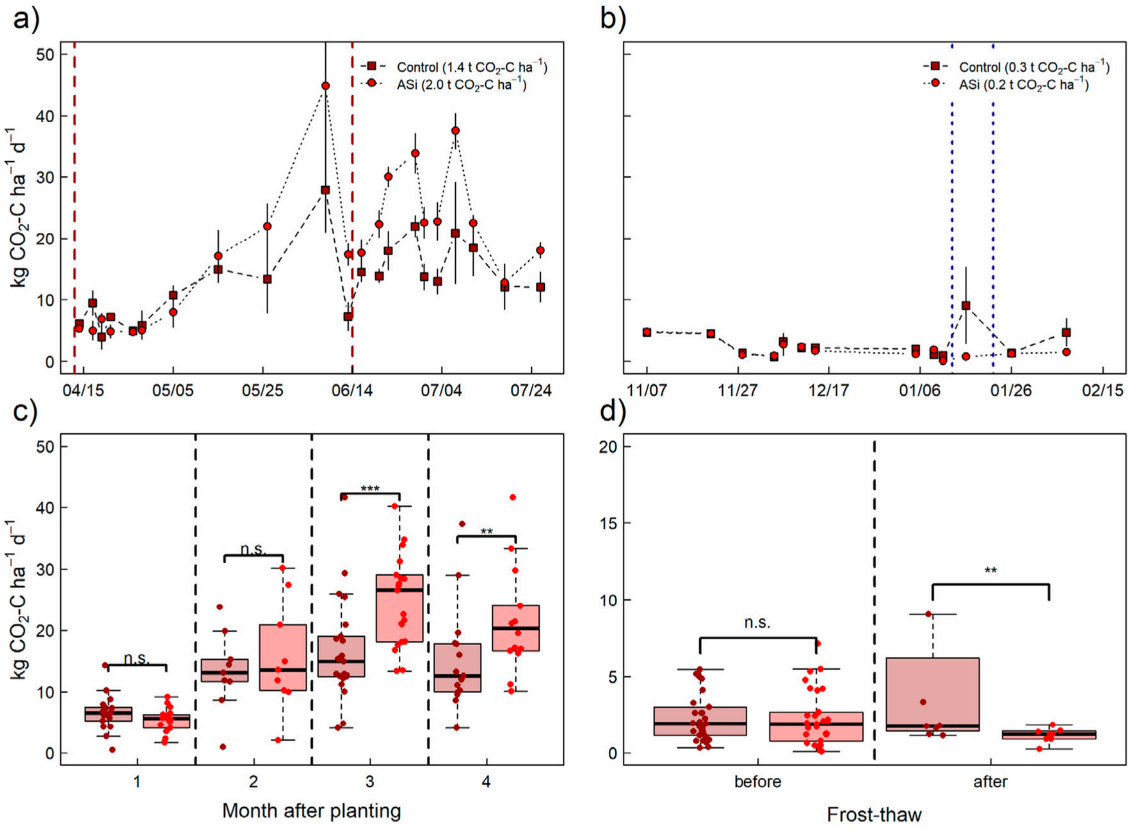

FIGURE 4
Results of periodically measured CO_2 emissions (kg CO_2-C ha^{-1} d^{-1}) for C (light red dots) and Si (dark red dots) during the **(A)** crop growth and **(B)** following fallow period in 2023 and 2023/2024, respectively. Error bars indicate ±SE. (Figures 3C, D) shows boxplots of CO_2 emissions grouped by period after planting (summer period) and before **(C)** vs. after frost-thaw **(D)** (winter period). Significant differences (Wilcoxon-test) between the Treatments within each group are indicated by asterisks (p-value: *** < 0.01, ** < 0.05, * < 0.1, n.s. > 0.1).

limits soil microorganisms by limited diffusion and the reduced supply of resources, such as organic N, to soil organisms (Schimel, 2018). Increased soil water content after ASi fertilization can therefore be expected to increase plant N availability via increased microbial N turnover. Finally, ASi fertilization might directly affect N availability: ASi dissolution generates silicic acid ($Si(OH)_4$) that is likely to compete for binding sites with NH_4^+, therefore increasing NH_4^+ availability in soil. This competition could increase the concentration of bioavailable NH_4^+ in the soil solution, similar to the observed mobilization of P by ASi (Schaller et al., 2019; Schaller et al., 2022). While nitrate (NO_3^-) is often the dominant form of plant-usable N in agriculture, an increase in bioavailable NH_4^+ through ASi application could still contribute to plant nutrition. Finally, we found a decrease in soil pH in the ASi fertilized plots. The soil pH of the main regulators of soil N_2O fluxes (Stehfest and Bouwman, 2006; Jamali et al., 2016; Hénault et al., 2019), affecting soil microbial community composition and activity. On the one hand, the moderately acidic conditions observed in ASi fertilization might have inhibited the nitrification and denitrification process and thus lowered the N_2O flux compared to the control. In acidic conditions, it is generally believed that the size and activity of nitrifying and denitrifying communities is reduced (Šimek et al., 2002; Park et al., 2018; Jadeja et al., 2021). It is likely that all three mentioned processes contributed to increased N and P availability in the present study, finally resulting in increased plant performance under ASi fertilization and greater depletion of the available N pool. Our data shows indeed a higher N uptake by crops following both fertilization events, which indicates less N availability in soils for microbial N_2O formation (Butterbach-Bahl et al., 2013). The observed reduction in N_2O emissions following ASi amendment started approximately 2 weeks after N fertilizer application. This time lag potentially reflects the time required for plants in the ASi treatment to enhance their N uptake, leading to a subsequent depletion of soil N available for microbial processes like nitrification and denitrification. While we cannot show reduced N availability directly, we indeed observed a higher N uptake by crops following both fertilization events (Figure 2B). The stronger reduction in N_2O emissions due to ASi after the first N-fertilization compared to the second N-fertilization event can be explained by the respective growing stage as the first N-fertilization took place at the time of maximum requirement of crops whereas the second N-fertilization took place at grain filling where crop N demand decreases (Delogu et al., 1998).

N_2O emissions during the fallow period were slightly higher for ASi compared to the control. However, summer exhibited clear distinctions, with ASi fertilization leading to reduced N_2O emissions compared to the control. This seasonal disparity suggests that plant performance may be a key driver of the observed differences in N_2O

emissions. Supporting this, the time point coinciding with the highest plant N uptake in the ASi treatment also corresponded with the most pronounced reduction in N_2O emissions. Further, our study revealed a positive correlation between N_2O emissions and soil moisture during the summer months, but not during winter. This seasonal disparity can likely be attributed to the strong influence of soil temperature on microbial activity. Microbial processes responsible for N_2O production, such as nitrification and denitrification, are significantly temperature-dependent (Davidson et al., 1991). During winter, when soil temperatures typically decline, these microbial activities are likely suppressed, leading to minimal N_2O emissions regardless of soil moisture content. The difference in soil pH between ASi treatment and control might be explained by higher microbial activity (due to potentially more root exudates and faster decomposition of organic matter), increased nitrification, and to a minor share by release of the weakly buffered silicic acid.

We could not directly verify our initial hypothesis that ASi fertilization supports nitrification through increasing soil moisture. No enhanced soil moisture was found for the ASi treatment compared to the control treatment during the winter as well as summer period for volumetric (VWC) as well as gravimetric water content (GWC; Figure 1; Table 1). In fact, especially during the summer period, VWC as well as GWC were slightly lower for ASi compared to control. The reason for this is most likely the increased biomass growth at the ASi treatment also increasing water demand, thus lowering soil water content for ASi compared to Control. However, soil moisture is not directly related to plant available water as hydraulic conductivity is strongly affected by ASi enhancing the matric potential at any soil water content (Schaller et al., 2020a). However, plants seem to be able to get access to this water decreasing plant water stress (Zarebanadkouki et al., 2024) potentially increasing biomass production (Schaller et al., 2023).

Overall, N uptake per ha was around 150 kg for ASi -treated, and only 67 kg for control plots. Considering that 125 kg N ha-1 were fertilized and that in agricultural systems, only about 50% of the N taken up by annual crops is current-year fertilizer derived (Gardner and Drinkwater, 2009; Yan et al., 2020) this indicates that large amounts of N were derived from soil organic matter in the ASi treatment. It is possible that the increased plant growth under ASi fertilization enhanced root derived C input which in turn induced rhizosphere priming, i.e., a short term increase in soil organic matter (SOM) decomposition caused by addition of easily available C from the root to the soil (Kuzyakov, 2002). Priming is positively related to gross N mineralization and uptake (Holz et al., 2023) and in particular to uptake of SOM-derived N (Pausch et al., 2024). The observation of a significant proportion of SOM-derived N in ASi-treated plants could potentially be attributed to enhanced rhizosphere priming effects triggered by ASi application. While this study did not separate plant-derived CO_2 from soil-derived CO_2, crucial for calculating rhizosphere priming effects, the observed increase in total CO_2 emissions from ASi-fertilized plants suggests ASi fertilization stimulated soil carbon turnover, potentially including rhizosphere priming. The increased CO_2 emissions due to ASi fertilization showed highest difference compared to the control treatment during the time of shoot elongation (Figure 4). Such increased CO_2 emissions due to ASi can be explained by the higher biomass production as increased root activity will lead to increased root and microbial respiration. However, as the enhanced plant growth in the ASi treatment will also increase C input by the plants, this does not necessarily indicate a negative C budget for the ASi treatment compared to the control. In a similar study for wheat grown at the same site during 2022, it could be shown that ASi addition compared to no ASi addition actually even resulted in a small C sink (Schaller et al., 2023). In this study it was deduced that both, the storage of CO_2 as carbonates and the sorption or binding of organic carbon by aggregates are probably insufficient to cause such effects over this short investigation period. Similarly, the storage of occluded organic carbon in phytoliths was mentioned to be unlikely to be responsible. Instead, the most probable cause argued was the increased C input from root biomass and root exudates during plant growth, which can be inferred from the increased aboveground biomass formation following ASi fertilization as shown in the study. Future studies should hence focus on longer term investigations and C pool separation in order to quantify the effect of ASi fertilization on the C budget and its causes.

To obtain a more comprehensive understanding of the impact of ASi fertilization on N_2O emissions from these poor soils, future research should consider multi-year experiments. This would allow for the incorporation of interannual variability and potentially capture the post-harvest period. Also the inclusion of periodic no-N fertilization treatments alongside ASi application and control groups would provide valuable insights. By comparing N_2O emissions across these treatments, researchers could isolate the specific effect of ASi on N use efficiency and its subsequent influence on N_2O production. Additionally, the study design of the present study did not allow us to determine which nutrient was most limiting for plant growth in the control treatment or to isolate which nutrient responded more strongly to ASi application and by which processes the nutrient availability was affected. To elucidate these questions, a future experiment employing a three-factorial design with ASi, N, and P fertilization as separate factors would be necessary.

Overall, we showed that ASi fertilization reduced N_2O emissions from a poor agricultural soil by over 30% compared to control plots without ASi fertilization. This reduction can likely be explained by the influence, ASi has on soil properties, potentially including enhanced plant-available water and increased microbial N turnover. Peak reduction in N_2O coincided with periods of high crop N demand, highlighting the critical role of plant performance. To obtain a more comprehensive understanding of the impact of ASi fertilization on N_2O emissions from these poor soils, future research should consider multi-year experiments including in particular measurements soil microbial activity and microbial community dynamics related to N turnover. This would allow not only for the incorporation of inter-annual variability but also to verify in a detail the underlying mechanisms. Also the In review inclusion of periodic no-N fertilization treatments alongside ASi application and control groups would provide valuable insights. By comparing N_2O emissions across these treatments, researchers could isolate the specific effect of ASi on N use efficiency and its subsequent influence on N_2O production. Additionally, the study design of the present study did not allow us to determine which nutrient was most limiting for plant growth in the control treatment or to isolate which nutrient responded more strongly to ASi application and by which processes the nutrient availability was affected. To elucidate these questions, a future experiment employing a three-factorial design with ASi, N, and P fertilization as separate factors would be necessary. In conclusion, ASi fertilization is a promising management practice for sustainable agriculture. By mitigating N losses while at the same time improving plant growth, ASi fertilization could be beneficial for both, the environment but also for crop production.

Data availability statement

All data generated and analyzed during this study will be freely available through https://doi.org/10.4228/zalf-km5x-g581 repository. Researchers interested in accessing the data can retrieve it using the provided DOI link. Additional details or requests can be directed to the corresponding author.

Author contributions

MHf: Conceptualization, Data curation, Software, Supervision, Validation, Visualization, Writing–review and editing. OD: Formal Analysis, Methodology, Writing–review and editing. IZ: Formal Analysis, Methodology, Writing–review and editing. WA-H: Formal Analysis, Writing–review and editing. MD: Project administration, Writing–review and editing. MS: Formal Analysis, Writing–review and editing. MHl: Writing–original draft, Writing–review and editing. JS: Conceptualization, Funding acquisition, Project administration, Writing–review and editing.

Funding

The author(s) declare that financial support was received for the research, authorship, and/or publication of this article. This research has been supported by the Leibniz Society Germany for their funding through the Leibniz Cooperative Excellence program (K378/2021) awarded to JS.

Acknowledgments

Special thanks goes to Yvonne Ayaribil and Shrijana Vaidya for their support during gas exchange measurements and the ZALF Research Station Müncheberg for their consistent support by managing the established field trail. We also thank the team of the central lab of ZALF for soil and biomass analysis.

Conflict of interest

The authors declare that the research was conducted in the absence of any commercial or financial relationships that could be construed as a potential conflict of interest.

Generative AI statement

The author(s) declare that no Generative AI was used in the creation of this manuscript.

Publisher's note

References

Badr, O., and Probert, S. (1993). Environmental impacts of atmospheric nitrous oxide. *Appl. energy* 44, 197–231. doi:10.1016/0306-2619(93)90018-k

Bouwman, A., Boumans, L., and Batjes, N. (2002). Emissions of N_2O and NO from fertilized fields: summary of available measurement data. *Glob. Biogeochem. cycles* 16, 6-1-6–13. doi:10.1029/2001gb001811

Butterbach-Bahl, K., Baggs, E. M., Dannenmann, M., Kiese, R., and Zechmeister-Boltenstern, S. (2013). Nitrous oxide emissions from soils: how well do we understand the processes and their controls? *Philosophical Trans. R. Soc. B Biol. Sci.* 368, 20130122. doi:10.1098/rstb.2013.0122

Chadwick, D., Cardenas, L., Misselbrook, T., Smith, K., Rees, R., Watson, C., et al. (2014). Optimizing chamber methods for measuring nitrous oxide emissions from plot-based agricultural experiments. *Eur. J. Soil Sci.* 65, 295–307. doi:10.1111/ejss.12117

Charteris, A. F., Chadwick, D. R., Thorman, R. E., Vallejo, A., De Klein, C. A., Rochette, P., et al. (2020). Global Research Alliance N_2O chamber methodology guidelines: recommendations for deployment and accounting for sources of variability. *J. Environ. Qual.* 49, 1092–1109. doi:10.1002/jeq2.20126

Clymans, W., Struyf, E., Govers, G., Vandevenne, F., and Conley, D. (2011). Anthropogenic impact on amorphous silica pools in temperate soils. *Biogeosciences* 8, 2281–2293. doi:10.5194/bg-8-2281-2011

Davidson, E., Hart, S., Shanks, C., and Firestone, M. (1991). Measuring gross nitrogen mineralization, and nitrification by ^{15}N isotopic pool dilution in intact soil cores. *J. Soil Sci.* 42, 335–349. doi:10.1111/j.1365-2389.1991.tb00413.x

Delogu, G., Cattivelli, L., Pecchioni, N., De Falcis, D., Maggiore, T., and Stanca, A. (1998). Uptake and agronomic efficiency of nitrogen in winter barley and winter wheat. *Eur. J. Agron.* 9, 11–20. doi:10.1016/s1161-0301(98)00019-7

Din-Iso-10694 (1995). Soil quality - determination of organic and total carbon after dry combustion (elementary analysis) (ISO 10694:1995). *Berl. Dtsch. Inst. für Norm.*

Galloway, J. N., Leach, A. M., Bleeker, A., and Erisman, J. W. (2013). A chronology of human understanding of the nitrogen cycle. *Philosophical Trans. R. Soc. B Biol. Sci.* 368, 20130120. doi:10.1098/rstb.2013.0120

Gardner, J. B., and Drinkwater, L. E. (2009). The fate of nitrogen in grain cropping systems: a meta-analysis of ^{15}N field experiments. *Ecol. Appl.* 19, 2167–2184. doi:10.1890/08-1122.1

Hart, S. C., Stark, J. M., Davidson, E. A., and Firestone, M. K. (1994). Nitrogen mineralization, immobilization, and nitrification. *Methods soil analysis Part 2 Microbiol. Biochem. Prop.* 5, 985–1018. doi:10.2136/sssabookser5.2.c42

Hénault, C., Bourennane, H., Ayzac, A., Ratié, C., Saby, N., Cohan, J.-P., et al. (2019). Management of soil pH promotes nitrous oxide reduction and thus mitigates soil emissions of this greenhouse gas. *Sci. Rep.* 9, 20182–20211. doi:10.1038/s41598-019-56694-3

Hoffmann, M., Pehle, N., Huth, V., Jurisch, N., Sommer, M., and Augustin, J. (2018). A simple method to assess the impact of sealing, headspace mixing and pressure vent on airtightness of manually closed chambers. *J. Plant Nutr. Soil Sci.* 181, 36–40. doi:10.1002/jpln.201600299

Holz, M., Paterson, E., and Pausch, J. (2023). Rhizosphere carbon priming: a plant mechanism to enhance soil nitrogen accessibility? *Plant Soil* 488, 175–185. doi:10.1007/s11104-023-05979-8

Huth, V., Hoffmann, M., Bereswill, S., Popova, Y., Zak, D., and Augustin, J. (2018). The climate warming effect of a fen peat meadow with fluctuating water table is reduced by young alder trees. *Mires and Peat* 21. doi:10.1002/jpln.201600493

Ipcc (2013). *Climate change 2013: the physical science basis. Contribution of working group I to the fifth assessment report of the intergovernmental panel on climate change*. Cambridge, United Kingdom and New York, NY, USA: Cambridge University Press.

Jadeja, A., Hirpara, D., Vekaria, L., and Sakarvadia, H. (2021). *Soil fertility and nutrient management: a way to sustainable agriculture*. taylor and francis.

Jamali, H., Quayle, W., Scheer, C., Rowlings, D., and Baldock, J. (2016). Effect of soil texture and wheat plants on N_2O fluxes: a lysimeter study. *Agric. For. meteorology* 223, 17–29. doi:10.1016/j.agrformet.2016.03.022

Katz, O., Puppe, D., Kaczorek, D., Prakash, N. B., and Schaller, J. (2021). Silicon in the soil–plant continuum: intricate feedback mechanisms within ecosystems. *Plants* 10, 652. doi:10.3390/plants10040652

Kendrick, K. J., and Graham, R. C. (2004). Pedogenic silica accumulation in chronosequence soils, southern California. *Soil Sci. Soc. Am. J.* 68, 1295–1303. doi:10.2136/sssaj2004.1295

Kuzyakov, Y. (2002). Review: factors affecting rhizosphere priming effects. *J. Plant Nutr. Soil Sci.* 165, 382–396. doi:10.1002/1522-2624(200208)165:4

Lassaletta, L., Billen, G., Garnier, J., Bouwman, L., Velazquez, E., Mueller, N. D., et al. (2016). Nitrogen use in the global food system: past trends and future trajectories of agronomic performance, pollution, trade, and dietary demand. *Environ. Res. Lett.* 11, 095007. doi:10.1088/1748-9326/11/9/095007

Lebauer, D. S., and Treseder, K. K. (2008). Nitrogen limitation of net primary productivity in terrestrial ecosystems is globally distributed. *Ecology* 89, 371–379. doi:10.1890/06-2057.1

Liu, S., Chi, Q., Cheng, Y., Zhu, B., Li, W., Zhang, X., et al. (2019). Importance of matching soil N transformations, crop N form preference, and climate to enhance crop yield and reducing N loss. *Sci. Total Environ.* 657, 1265–1273. doi:10.1016/j.scitotenv.2018.12.100

Livingston, G., and Hutchinson, G. (1995). "Enclosure-based measurement of trace gas exchange: applications and sources of error," in *Biogenic trace gases: measuring emissions from soil and water* 51, 14–51.

Loftfield, N., Flessa, H., Augustin, J., and Beese, F. (1997). Automated gas chromatographic system for rapid analysis of the atmospheric trace gases methane, carbon dioxide, and nitrous oxide. *J. Environ. Qual.* 26, 560–564. doi:10.2134/jeq1997.00472425002600020030x

Ma, J. F., and Takahashi, E. (2002). *Soil, fertilizer, and plant silicon research in Japan*. Elsevier.

Marschner, H. (2003). *Mineral nutrition of higher plants*. London: Academic Press.

Mbow, C., Rosenzweig, C., Barioni, L. G., Benton, T. G., Shukla, P., Skea, J., et al. (2019). Climate change and land. *IPCC SPECIAL Rep. Glob. Warming 1.5 oC*, 1–200. Chapter 5: food security.

Mosier, A. R., Halvorson, A. D., Reule, C. A., and Liu, X. J. (2006). Net global warming potential and greenhouse gas intensity in irrigated cropping systems in northeastern Colorado. *J. Environ. Qual.* 35, 1584–1598. doi:10.2134/jeq2005.0232

Myrold, D. D., and Tiedje, J. M. (1986). Simultaneous estimation of several nitrogen cycle rates using 15N: theory and application. *Soil Biol. Biochem.* 18, 559–568. doi:10.1016/0038-0717(86)90076-3

Norton, J. M., and Schimel, J. (2011). Nitrogen mineralization immobilization turnover. *Handb. soil Sci.*

Pareja-Sánchez, E., Cantero-Martínez, C., Álvaro-Fuentes, J., and Plaza-Bonilla, D. (2020). Impact of tillage and N fertilization rate on soil N_2O emissions in irrigated maize in a Mediterranean agroecosystem. *Agric. Ecosyst. and Environ.* 287, 106687. doi:10.1016/j.agee.2019.106687

Park, S. H., Lee, B. R., Jung, K. H., and Kim, T. H. (2018). Acidification of pig slurry effects on ammonia and nitrous oxide emissions, nitrate leaching, and perennial ryegrass regrowth as estimated by ^{15}N-urea flux. *Asian-Australasian J. animal Sci.* 31, 457–466. doi:10.5713/ajas.17.0556

Pausch, J., Holz, M., Zhu, B., and Cheng, W. (2024). Rhizosphere priming promotes plant nitrogen acquisition by microbial necromass recycling. *Plant, Cell and Environ.* 47, 1987–1996. doi:10.1111/pce.14858

Pradhan, P., Fischer, G., Van Velthuizen, H., Reusser, D. E., and Kropp, J. P. (2015). Closing yield gaps: how sustainable can we be? *PloS one* 10, e0129487. doi:10.1371/journal.pone.0129487

Puppe, D., Kaczorek, D., Buhtz, C., and Schaller, J. (2023). The potential of sodium carbonate and Tiron extractions for the determination of silicon contents in plant samples—a method comparison using hydrofluoric acid digestion as reference. *Front. Environ. Sci.* 11, 1145604. doi:10.3389/fenvs.2023.1145604

Puppe, D., Kaczorek, D., Schaller, J., Barkusky, D., and Sommer, M. (2021). Crop straw recycling prevents anthropogenic desilication of agricultural soil-plant systems in the temperate zone – results from a long-term field experiment in NE Germany. *Geoderma* 403, 115187. doi:10.1016/j.geoderma.2021.115187

Ravishankara, A., Daniel, J. S., and Portmann, R. W. (2009). Nitrous oxide (N_2O): the dominant ozone-depleting substance emitted in the 21st century. *science* 326, 123–125. doi:10.1126/science.1176985

Reay, D. S., Davidson, E. A., Smith, K. A., Smith, P., Melillo, J. M., Dentener, F., et al. (2012). Global agriculture and nitrous oxide emissions. *Nat. Clim. change* 2, 410–416. doi:10.1038/nclimate1458

Reithmaier, G. M. S., Knorr, K. H., Arnhold, S., Planer-Friedrich, B., and Schaller, J. (2017). Enhanced silicon availability leads to increased methane production, nutrient and toxicant mobility in peatlands. *Sci. Rep.* 7, 8728. doi:10.1038/s41598-017-09130-3

Saccone, L., Conley, D. J., Koning, E., Sauer, D., Sommer, M., Kaczorek, D., et al. (2007). Assessing the extraction and quantification of amorphous silica in soils of forest and grassland ecosystems. *Eur. J. Soil Sci.* 58, 1446–1459. doi:10.1111/j.1365-2389.2007.00949.x

Schaller, J., Cramer, A., Carminati, A., and Zarebanadkouki, M. (2020a). Biogenic amorphous silica as main driver for plant available water in soils. *Sci. Rep.* 10, 2424. doi:10.1038/s41598-020-59437-x

Schaller, J., Fauchere, S., Joss, H., Obst, M., Goeckede, M., Planer-Friedrich, B., et al. (2019). Silicon increases the phosphorus availability of Arctic soils. *Sci. Rep.* 9, 449. doi:10.1038/s41598-018-37104-6

Schaller, J., Frei, S., Rohn, L., and Gilfedder, B. S. (2020b). Amorphous silica controls water storage capacity and phosphorus mobility in soils. *Front. Environ. Sci.* 8. doi:10.3389/fenvs.2020.00094

Schaller, J., Macagga, R., Kaczorek, D., Augustin, J., Barkusky, D., Sommer, M., et al. (2023). Increased wheat yield and soil C stocks after silica fertilization at the field scale. *Sci. Total Environ.* 887, 163986. doi:10.1016/j.scitotenv.2023.163986

Schaller, J., Puppe, D., Kaczorek, D., Ellerbrock, R., and Sommer, M. (2021a). Silicon cycling in soils revisited. *Plants* 10, 295. doi:10.3390/plants10020295

Schaller, J., Scherwietes, E., Gerber, L., Vaidya, S., Kaczorek, D., Pausch, J., et al. (2021b). Silica fertilization improved wheat performance and increased phosphorus concentrations during drought at the field scale. *Sci. Rep.* 11, 20852. doi:10.1038/s41598-021-00464-7

Schaller, J., Wu, B., Amelung, W., Hu, Z., Stein, M., Lehndorff, E., et al. (2022). Silicon as a potential limiting factor for phosphorus availability in paddy soils. *Sci. Rep.* 12, 16329. doi:10.1038/s41598-022-20805-4

Schimel, J. P. (2018). Life in dry soils: effects of drought on soil microbial communities and processes. *Annu. Rev. Ecol. Evol. Syst.* 49, 409–432. doi:10.1146/annurev-ecolsys-110617-062614

Seiffert, S., Kaselowsky, J., Jungk, A., and Claassen, N. (1995). Observed and calculated potassium uptake by maize as affected by soil water content and bulk density. *Agron. J.* 87, 1070–1077. doi:10.2134/agronj1995.00021962008700060007x

Shcherbak, I., Millar, N., and Robertson, G. P. (2014). Global metaanalysis of the nonlinear response of soil nitrous oxide (N_2O) emissions to fertilizer nitrogen. *Proc. Natl. Acad. Sci.* 111, 9199–9204. doi:10.1073/pnas.1322434111

Šimek, M., Jı´Šová, L., and Hopkins, D. W. (2002). What is the so-called optimum pH for denitrification in soil? *Soil Biol. Biochem.* 34, 1227–1234. doi:10.1016/s0038-0717(02)00059-7

Stehfest, E., and Bouwman, L. (2006). N_2O and NO emission from agricultural fields and soils under natural vegetation: summarizing available measurement data and modeling of global annual emissions. *Nutrient Cycl. Agroecosyst.* 74, 207–228. doi:10.1007/s10705-006-9000-7

Sutton, M. A., Oenema, O., Erisman, J. W., Leip, A., Van Grinsven, H., and Winiwarter, W. (2011). Too much of a good thing. *Nature* 472, 159–161. doi:10.1038/472159a

Tallec, T., Béziat, P., Jarosz, N., Rivalland, V., and Ceschia, E. (2013). Crops' water use efficiencies in temperate climate: comparison of stand, ecosystem and agronomical approaches. *Agric. For. Meteorology* 168, 69–81. doi:10.1016/j.agrformet.2012.07.008

Van Groenigen, J., Huygens, D., Boeckx, P., Kuyper, T. W., Lubbers, I., Rütting, T., et al. (2015). The soil N cycle: new insights and key challenges. *Soil* 1, 235–256. doi:10.5194/soil-1-235-2015

Vitousek, P. M., and Howarth, R. W. (1991). Nitrogen limitation on land and sea - how can it occur. *Biogeochemistry* 13, 87–115. doi:10.1007/bf00002772

Yan, M., Pan, G., Lavallee, J. M., and Conant, R. T. (2020). Rethinking sources of nitrogen to cereal crops. *Glob. change Biol.* 26, 191–199. doi:10.1111/gcb.14908

Zarebanadkouki, M., Al Hamwi, W., Abdalla, M., Rahnemaie, R., and Schaller, J. (2024). The effect of amorphous silica on soil–plant–water relations in soils with contrasting textures. *Sci. Rep.* 14, 10277. doi:10.1038/s41598-024-60947-1

Zarebanadkouki, M., Fink, T., Benard, P., and Banfield, C. C. (2019). Mucilage facilitates nutrient diffusion in the drying rhizosphere. *Vadose Zone J.* 18, 1–13. doi:10.2136/vzj2019.02.0021

Zhang, J., Cai, Z., and Müller, C. (2018). Terrestrial N cycling associated with climate and plant-specific N preferences: a review. *Eur. J. Soil Sci.* 69, 488–501. doi:10.1111/ejss.12533